Vol. 23, No. 1(2024) Bio24139
Revista Mexicana de Ingeniería Química

Secondary structure by circular dichroism spectroscopy of β-*N*-acetylglucosaminidase from *Lecanicillium lecanii* and its relationship with hydrolytic and transglycosylation activities at different pH values

Estructura secundaria por espectroscopía de dicroísmo circular de la β-*N*-acetilglucosaminidasa de *Lecanicillium lecanii* y su relación con su actividades hidrolítica y de transglicosilación a diferentes valores de pH

J. Rojas-Osnaya[1,2,3], S. R. Tello-Solís[2*], K. Shirai[1*]

[1] *1Universidad Autónoma Metropolitana-Iztapalapa, Departamento de Biotecnología, Laboratorio de Biopolímeros y Planta Piloto de Bioprocesos de Alimentos y Productos Agroindustriales.* [2] *Departamento de Química, Área de Biofisicoquímica. Av. San Rafael Atlixco No. 186, Iztapalapa 09310, México City, México.*

[3] *Universidad Autónoma Metropolitana-Cuajimalpa. Departamento de Ciencias Naturales. Laboratorio de Biofisicoquímica. Av. Vasco de Quiroga 4871. Col. Santa Fe Cuajimalpa, Mexico City.C.P.05348. México.*

Received: August 29, 2023; Accepted: January 16, 2023

Abstract

N-acetylglucosaminidase produced and purified from *Lecanicillium lecanii* was analyzed using circular dichroism spectroscopy. The enzyme is mainly an ($\alpha + \beta$)-type protein, having 76 % α-helix, 4 % parallel β-sheet, 2 % antiparallel β-sheet, 8 % β-turns, and 10 % unordered structure at pH 10 (condition leading to the highest secondary structure content, 100% ellipticity). The circular dichroism spectra analysis as a function of pH shows a decrease in α-helix content at pH < 8. The structure-activity relationship as a function of pH to hydrolytic or transglycosylation reactions was studied. The maximum transglycosylation activity for four donor substrates was at pH 7, while hydrolytic activity was at pH 6. The highest activity pH values do not correspond to the maximum percentage of ellipticity for both. The maximum hydrolytic or transglycosylation activity observed is associated with conformational changes in the enzyme when pH diminishes.

Keywords: *N*-acetylglucosaminidase, *Lecanicillium lecanii*, circular dichroism, hydrolytic, transglycosylation.

Resumen

La *N*-acetilglucosaminidasa producida y purificada a partir de *Lecanicillium lecanii* se analizó mediante espectroscopía de dicroísmo circular. La enzima es principalmente una proteína de tipo ($\alpha + \beta$), que tiene 76 % de hélice α, 4 % de lámina β paralela, 2 % de lámina β antiparalela, 8 % de giros β y 10 % de estructura desordenada a pH 10 (condición que conduce al mayor contenido de estructura secundaria, 100% de elipticidad). El análisis de los espectros de dicroísmo circular en función del pH muestra una disminución en el contenido de hélice α a pH < 8. Se estudió la relación estructura-actividad en función del pH para reacciones hidrolíticas o de transglicosilación. La máxima actividad de transglicosilación para los cuatro sustratos donadores fue a pH 7, mientras que para la actividad hidrolítica fue a pH 6. Los valores de pH de mayor actividad no corresponden al porcentaje máximo de elipticidad en ambos casos. La máxima actividad hidrolítica o de transglicosilación observada está asociada con cambios conformacionales de la enzima cuando el pH disminuye.

Palabras clave: *N*-acetilglucosaminidasa, *Lecanicillium lecanii*, dicroísmo circular, hidrolítica, transglicosilación.

*Corresponding authors. *E-mail*: srts@xanum.uam.mx (Tello-Solís) and smk@xanum.uam.mx(Shirai);
https://doi.org/10.24275/rmiq/Bio24139
ISSN:1665-2738, *issn-e*: 2395-8472

1 Introduction

Chitinases are glycosyl hydrolase enzymes capable of hydrolyzing the β-1, 4 bonds of chitin, which is a biopolymer composed of *N*-acetyl-D-glucosamine (GlcNAc) units (Zapata-Luna *et al*., 2023). Chitinases can also hydrolyze chitosan (non-toxic biopolymer) (Herrrera Gonzalez *et al*., 2023). Chitinases are classified into endochitinase (EC 3.2.1.1.14) and exo-types of β-*N*-acetylglucosaminidase, chitobiase, or β-*N*-acetylglucosaminidases (Hex) (EC 3.2.1.52) (Yang *et al*., 2014). Chitinases are distributed in various organisms, such as insects, plants, bacteria, and fungi. Fungal chitinases belong to the glycosyl hydrolase 18 families (GH18), divided into subfamilies A, B, and C, according to their sequence similarity and enzymatic activities. The subgroups A and B contained all the identified fungal chitinases in the literature. These chitinases have a range of molecular masses between 30-90 kDa, whereas subgroup C comprised a novel group of chitinases with high molecular masses of 140-170 kDa. Chitinases from subgroups B and C have carbohydrate-binding modules, and subgroup A does not present this characteristic; however, they have an *N*-terminal signal peptide, indicating they are extracellular proteins (Seidl *et al*., 2008; Adrangi *et al*., 2013). GH18 hydrolyzes the glycosidic linkage through a double displacement mechanism with the net retention of the configuration at the anomeric carbon (Umemoto *et al*., 2015). In addition to their hydrolytic activity, some chitinases can carry out transglycosylation activity (TGA) by transferring an oligosaccharide to a suitable acceptor to form a new glycosidic bond (Li *et al*., 2008). The donor and acceptor saccharides form a new glycosidic bond, leading to a TGA when the water molecule is outcompeted by the acceptor molecule (Mallakuntla *et al*., 2020). TGA occurs through two steps: an acceptor molecule binds to the catalytic cleft, and then the glycosidic linkage is newly generated (Taira *et al*., 2010).

Several techniques are applied to obtain information on the structural conformations of proteins and peptides. Among them is circular dichroism (CD) spectroscopy, a powerful technique that provides information about the molecular structure of proteins or polypeptides in a solution. Circular dichroism spectroscopy measures the differential absorption of left and right circularly polarized light according to the molecules that exhibit optical activity (not having a symmetrical plane and not being superimposable with their mirror image). The chromophore of proteins of interest included the peptide bond (240-190 nm), aromatic groups (260-320 nm), and each amino acid, and, respectively, each one tends to have a characteristic wavelength profile, such as tryptophan at 290 nm, tyrosine at 275 nm, phenylalanine at 255 nm and disulfide bonds at 260 nm; in addition, other compounds in CD, such as flavins (300-500 nm) and cofactors close to 330 nm, can, also, be analyzed (Kelly *et al*., 2005). It has been reported that quinazoline alkaloids polonimides obtained from the fungus *Penicillium polonicum* function as inhibitors of chitinase activity. The configurations of these alkaloids were determined by the combination of nuclear overhauser effect (NOE), nuclear magnetic resonance (NMR), and CD (Guo *et al*., 2020). The analysis of circular dichroism spectra in the far ultraviolet region (240-190 nm) allows the estimation of the secondary structure content of proteins and electronic transitions between molecular orbitals in the ground and excited states (Greenfield, 2006). DICHROWEB is an online service that enables the deconvolution of CD spectra and quantifying the percentages of secondary structures present in the polypeptide chain such as alpha helix, antiparallel beta-sheet, parallel beta-sheet, and beta turns (Lobley *et al*., 2002; Whitmore *et al*., 2004). Hou *et al*. (2019) studied the effect of ultrasound on conformational changes and enzymatic activity of chitinase from *Streptomyces griseus*. The increase in random coil and beta-sheet affected the secondary structure's content. At the same time, the turns and alpha helix decreased when the chitinase was treated by ultrasound, improving the chitinase activity. To the best of our knowledge, this work is the first to report the study of the secondary structure of Hex from *L. lecanii* by CD and the relationship of the structure and hydrolytic and transglycosylation activities as a function of pH.

2 Materials and methods

2.1 Production and purification of Hex

The production and purification of Hex were carried out, as reported by Rojas-Osnaya *et al*. (2020). The production of Hex was carried out in a submerged culture by inoculation of 10^7 spores/mL of *Lecanicillium lecanii* strain ATCC 26854 in a 3 L bioreactor (Applikon BV, Netherlands) using a modified Czapeck culture medium at pH 6, 100 rpm of agitation, 1 vvm of aeration, and incubated at 25 °C for 144 h. For the purification of Hex, the submerged culture was centrifuged at 8000 rpm at 4 °C for 10 min (Thermo Scientific, Legend XTR, Waltham, Massachusetts, USA). The supernatant was processed using precipitation with ammonium sulfate, followed by molecular exclusion chromatography (SEC) and anion exchange chromatography (AEC). The chromatographies were performed in an FPLC (AKTA, GE Healthcare, Stockholm, Sweden).

Fractions with the highest hydrolytic Hex activity from AEC were lyophilized and stored at 4 °C for later use.

2.2 *Protein content and SDS-PAGE*

The Bradford method determined the protein content of the purified enzymatic fraction (Bradford, 1976). The fraction was subjected to electrophoresis under denaturing conditions (SDS-PAGE). The gel was stained by Coomassie Brilliant BlueG-250 (Bio-Rad, Catalog Number # 786-497). A broad range of SDS-PAGE molecular weights (Mw) standards were used as a reference.

2.3 *Hydrolytic activity and transglycosylation activity*

The hydrolytic activity was determined using 200 μL of the enzyme (concentration 40 μg/mL) added to 200 μL of p-nitrophenyl-β-*N*-acetylglucosamine (1 mg/mL) used as the substrate and 200 μL of 0.2 M citrate/phosphate buffer pH at range from 3 to 11 at 37 °C. An enzymatic unit was defined as the amount of enzyme that releases 1 μmol of p-nitrophenol per minute (Tronsmo and Harman, 1993).

TGA was carried out by using 4-methylumbelliferyl-*N*-acetyl-glucosaminide as the acceptor substrate and *N*-acetyl-D-glucosamine (GlcNAc), glucose (Glu), *N*-acetyl-D-Lactosamine (NaLac) or mannose (Man) as a donor substrate. 50 μL of each of the donor substrates (0.0004 M) was added to 50 μL of the enzyme (concentration 50 μg/mL (1×10^{-6} M) was added to 50 μL of 4-methylumbelliferyl-*N*-acetyl-glucosaminide (0.001 M) in 50 μL citrate/phosphate buffer 0.2 M in a range of pH from 4 to 11 at 37 °C. After aliquots of 10 μL were taken at 1.3 h, 200 μL of glycine buffer (0.15 M) at pH 10.5 was added. Fluorescence was determined using an excitation wavelength of 355 nm and emission wavelength of 460 nm in a multimode microplate reader (Tecan M1000 PRO, Männedorf Switzerland) (Li *et al*., 2008).

2.4 *Secondary structure of Hex by circular dichroism*

Hex solutions were prepared with a concentration of 0.012 - 0.030 mg/mL in acidified deionized water with HCl 1M or NaOH 1M in a solution containing 5 mM phosphate at different pH values (4-11) and 25 °C. For the experiments of CD, the protein concentration was estimated spectrophotometrically by measuring the absorbance of each Hex solution at 280nm (A_{280nm} = 2.65 $(mg/mL)^{-1} \cdot cm^{-1}$). CD spectra were obtained using a Jasco J-715 spectropolarimeter (Tokyo, Japan) calibrated with (+) -10-camphorsulphonic acid Kelly *et al*., (2005), with a wavelength of 240 to 190 nm

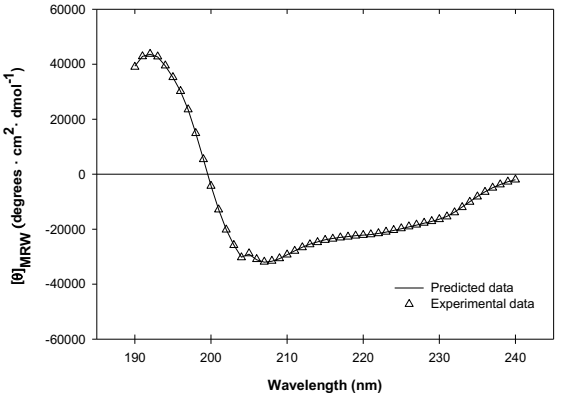

Fig.1. Hex CD spectrum of *L. lecanii* determined at pH 10 and 37 °C. Experimental data (Δ). Predicted data (-) was calculated with CDSSRT algorithm.

at 37 °C, using a 0.2 cm cell, each spectrum reported is the average of 5 consecutive scans. To estimate the secondary structure content of Hex, circular dichroism data was analyzed in the DICHROWEB (Whitmore and Wallace, 2008) database using the CDSSTR algorithm of Sreerama and Woody, (2000). The data were reported as a mean residue ellipticity ($[\theta]_{MRW}$) calculated by Eq.1.

$$[\theta]_{MRW} = \frac{\theta(MRW)}{10dc} \quad (1)$$

where $[\theta]_{MRW}$ is the mean residue ellipticity (degrees $\cdot$ cm$^2\cdot$ dmol^{-1}), MRW is the mean residue weight of 110 Da, θ is the ellipticity in millidegrees (m°), c is the protein concentration (mg/mL), and d is the pathlength in cm.

3 Results and discussion

3.1 *Effect of the pH on the secondary structure of Hex*

After purification, the protein showed a single band at 50 kDa on SDS-PAGE (Supplementary data 1). CD spectrum of Hex from *L. lecanii* at pH 10, and 25 °C in the far ultraviolet region 240-190 nm is shown in Fig.1. The spectrum showed a positive band at 195 nm as well as negative bands around 208 and 220 nm, Manavalan and Johnson (1983) reported that these bands are characteristics of proteins denominate $\alpha + \beta$ (separate α-helix and β-sheet rich regions), within this group is lysozyme, which is a protein that belongs to the family of glycosyl hydrolases. According to this, Makshakova *et al*. (2021) observed that the CD spectrum of lysozyme from chicken egg white presents these three signals, corroborating that they are $\alpha + \beta$ proteins, the structure of lysozyme is organized in two domains, one contains four alpha helix and the second contains three antiparallel beta

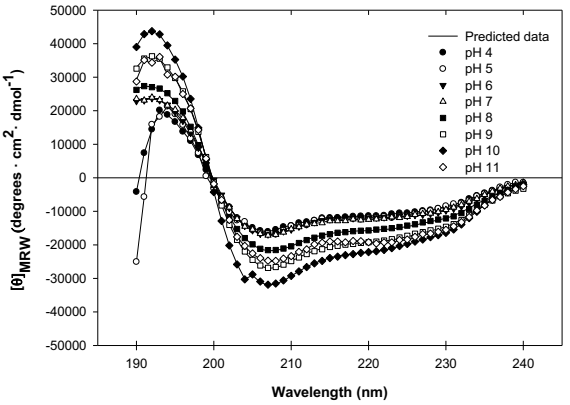

Fig.2. Hex CD spectra of *L. lecanii* determined at different pH values at 37 ºC. Predicted data (-) was calculated with CDSSRT algorithm.

sheets. To estimate the secondary structure content, the CD spectrum of Hex was analyzed by the CDSSRT algorithm available on Dichroweb (Whitmore and Wallace, 2008). This analysis produces a calculated curve that reproduces the experimental points of the CD spectrum of Hex (Fig. 1).

In Fig. 2, the analyzed and calculated Hex spectra at different pH values are seen, where the dichroism signal was observed to be at its maximum at 195 nm and two minimum, one at 208 and the other at 220 nm, being a deeper signal at 208 nm; therefore, a change in ellipticity can be inferred depending on the pH range. For alkaline conditions (pH 8 to 11), the ellipticity values increased at the signal of 195 nm, and the bands around 208 and 220 nm increase negatively. Wallace and Janes, (2001) reported that for an α-helix, the positive band around 195 nm and the negative band at 208 nm in CD spectra are assigned to $\pi_0 \rightarrow \pi^*$ transitions of polypeptide chains, and for negative bands above 200 nm are to $n \rightarrow \pi^*$ transitions. According to Lienemann *et al*. (2009), the chitinase from *Trichoderma harzianum* showed a deeper signal at 220 nm at pH 6.5 and 25 °C, resulting in more transitions $n \rightarrow \pi^*$.

Table 1 shows the estimation of the secondary structure of Hex at different pH values using the CDSSTR algorithm, where pHs 4, 5, 6, and 7, the alpha helix conformation is in the range of 47-53%, all beta-type contributions are in the order of 26-33%. In comparison, the irregular structure remains constant at 20% for alkaline pH 8-11; a considerable increase in the alpha helix structure is observed, greater than 60%, and a decrease in all beta-type and irregular structures.

The above changes were attributed to a possible rearrangement of the protein due to the presence or absence of hydrogen bonds or changes in electrostatic interactions (ion pairs), whose destabilization is by the ionic atmosphere of the solution (López-Arenas *et al*., 2006). The experimental data fit well with the predicted data, reflected in obtaining an NRMSD (normalized root mean square deviation) (Whitmore and Wallace. 2004) value lower than 0.1 in all the analyzed spectra. At pH below 7, the α-structure composition remains at values close to 50 %. In comparison, the alpha structure's percentage increases to 74 % at alkaline pH values, and the beta structure composition goes from 23 % to 9 %. For the turns, there are no considerable changes in the pH range (4-11). (Table 1). A plausible explanation for the increase in alpha structure can be attributed to hydroxyl ions that can destabilize the hydrogen bonds in the protein. As was reported by Halder *et al*. (2016) observed that the alteration of the pH destabilizes the non-covalent bonds of the structure of the chitinase from *Aeromonas hydrophila*.

3.2 *Effect of pH on the Conformation and Activities of Hex*

The effect of pH on the conformation and activities of Hex is shown in Fig. 3. Changes in the percentage of the signal of mean residue ellipticity at 195 nm as a reflection of all secondary structure functions of pH is shown in Fig. 3A, as we can see, the highest content of secondary structure was found at pH 10 (100 % of mean residue ellipticity).

Table 1. Contribution of the secondary structure of the Hex of *L. lecanii* at different pH values at 37 °C. Calculated by the CDSSRT Algorithm (Sreerama *et al*., 2000).

pH	α-helix (%)	β-sheet (%)		Turns (%)	Unordered (%)	Total (%)	NRMSD[a]
		parallel	antiparallel				
4	47	13	10	10	20	100	0.002
5	48	13	11	8	20	100	0.002
6	54	9	5	12	20	100	0.010
7	53	10	6	12	20	101	0.011
8	63	7	4	8	17	99	0.011
9	74	5	2	6	12	99	0.008
10	76	4	2	8	10	100	0.004
11	74	6	3	8	10	101	0.008

[a]Relative error calculated by the CDSSRT algorithm (Sreerama *et al*., 2000)

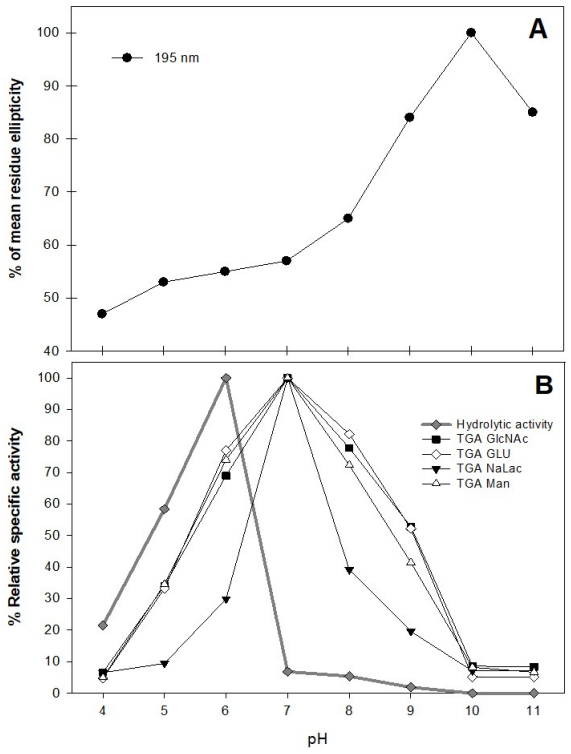

Fig.3. Effect of pH at 195 nm (A) and TGA and hydrolytic activities (B) of Hex from *L. lecanii*. The ellipticity values are expressed as percentages of the value estimated at pH 10 (100%).

At pH values 4 to 7, the percentage of global mean residue ellipticity is maintained close to 50%, suggesting a stabilization of the secondary structure after a considerable overall secondary structure change with increasing acidity of the solution from pH 10 to 7, presenting a decrease in the alpha helix structure (Table 1). For pH values > 10, the observed global conformational changes are minor. Fig. 3B shows the highest hydrolytic and TGA activities for the four donor substrates at different pH values, for pH 6 and 7 values do not correspond to the maximum % ellipticity when comparing Fig. 3A and 3B.

According to previous work by Rojas-Osnaya *et al*. (2020), the maximum hydrolytic activity and TGA were presented at pH 6 and 7, respectively. The present study indicates that, at these pH, the α and β structures do not present significant changes in their composition (Table 1), which suggests that the difference in activities is probably from the deprotonations of the amino acids (glutamic and aspartic acid) present in the active site of Hex. Furthermore, Fig 3A shows that for total conformational changes > 30%, the hydrolytic activity falls abruptly, which implies that the activity strongly depends on the conformation of the enzyme. At the same time, for TGA, this effect is not observed.

Conclusions

According to the CD spectra of Hex from *L. lecanii*, it is a protein that presents a secondary structure of the (α + β)-type, being present in a more significant proportion of the α-helix structure throughout the pH range studied. The CD spectra showed that pH 10 leads to the highest secondary structure content (100 % ellipticity). The maximum hydrolytic activity was found at pH 6, while for TGA, it was at pH 7 (for the four donor substrates). In both reactions studied, the pH value of maximum activity observed does not correspond to the pH value of maximum ellipticity due to conformational changes of the enzyme as a function of pH.

Acknowledgment

The authors thank the Secretary of Education, Science Technology and Innovation of México City (SECTEI) of the Government of México City for funding Project No. SECTEI/2023 and to the Conformation and Consolidation Program of Research Networks Project UAM ECOCISTA 11/2022 and Consejo Nacional de Ciencia y Tecnología (CONACyT) for funding and scholarship grant (JRO). Cuerpo Académico de Biofisicoquimica (SEP México) (SRTS).

References

Adrangi, S., Faramarzi, M. A. (2013). From bacteria to human: a journey into the world of chitinases. *Biotechnology Advances 31*(8), 1786-1795. https://doi.org/10.1016/j.biotechadv.2013.09.012

Bradford, N. J. A. B. (1976). A rapid and sensitive method for the quantitation of microgram quantities of a protein isolated from red cell membranes. *Anals of Biochemistry 72*(248), e254. https://doi.org/10.1016/0003-2697(76)90527-3

Greenfield, N. J. (2006). Using circular dichroism spectra to estimate protein secondary structure. *Nature Protocols 1*(6), 2876-2890. https:doi.org/10.1038/nprot.2006.202

Guo, X. C., Zhang, Y. H., Gao, W. B., Pan, L., Zhu, H. J., Cao, F. (2020). Absolute configurations and chitinase inhibitions of quinazoline-containing diketopiperazines from the marine-derived fungus *Penicillium polonicum*. *Marine Drugs 18*(9), 479. https://doi.org/10.3390/md18090479

Halder, S. K., Jana, A., Paul, T., Das, A., Ghosh, K., Pati, B. R., Mondal, K. C. (2016). Purification and biochemical characterization of chitinase of Aeromonas hydrophila SBK1 biosynthesized using crustacean shell. *Biocatalysis and Agricultural Biotechnology 5*, 211-218. https://doi.org/10.1016/j.bcab.2015.11.003

Herrera-González, J.A., Hernández-Sánchez, D.A., Bueno-Rojas, D.A., Ramos-Bell,S., Velázquez-Estrada, R.M., Bautista-Rosales, P.U., Gutiérrez-Martínez, P. (2022). Effect of commercial chitosan on *in vitro* inhibition of *Colletotrichum siamense*, fruit quality and elicitor effect on postharvest avocado fruit. *Revista Mexicana de Ingeniería Química 21*(1), 1-12. https://doi.org/10.24275/rmiq/Bio2706

Hou, F., Ma, X., Fan, L., Wang, D., Wang, W., Ding, T., Liu, D. (2019). Activation and conformational changes of chitinase induced by ultrasound. *Food Chemistry 285*, 355-362. https://doi.org/10.1016/j.foodchem.2019.01.180

Kelly, S. M., Jess, T. J., & Price, N. C. (2005). How to study proteins by circular dichroism. *Biochimica et Biophysica Acta (BBA)-Proteins and Proteomics 1751*(2), 119-139. https://doi.org/10.1016/j.bbapap.2005.06.005

Li, C., Huang, W., Wang, L. X. (2008). Chemoenzymatic synthesis of *N*-linked neoglycoproteins through a chitinase-catalyzed transglycosylation. *Bioorganic & Medicinal Chemistry 16*(18), 8366-8372. https://doi.org/10.1016/j.bmc.2008.08.042

Lienemann, M., Boer, H., Paananen, A., Cottaz, S., Koivula, A. (2009). Toward understanding of carbohydrate binding and substrate specificity of a glycosyl hydrolase 18 family (GH-18) chitinase from *Trichoderma harzianum*. *Glycobiology 19*(10), 1116-1126. https://doi.org/10.1093/glycob/cwp102

Lobley, A., Whitmore, L., Wallace, B. A. (2002). DICHROWEB: an interactive website for the analysis of protein secondary structure from circular dichroism spectra. *Bioinformatics 18*(1), 211-212. https://doi.org/10.1093/bioinformatics/18.1.211

López-Arenas, L., Solís-Mendiola, S., Padilla-Zúñiga, J., Hernández-Arana, A. (2006). Hofmeister effects in protein unfolding kinetics: Estimation of changes in surface area upon formation of the transition state. *Biochimica et Biophysica Acta (BBA)-Proteins and Proteomics 1764*(7), 1260-1267. https://doi.org/10.1016/j.bbapap.2006.05.006

Makshakova, O. N., Bogdanova, L. R., Faizullin, D. A., Ermakova, E. A., Zuev, Y. F., Sedov, I. A. (2021). Interaction-induced structural transformation of lysozyme and kappa-carrageenan in binary complexes. *Carbohydrate Polymers 252*, 117181. https://doi.org/10.1016/j.carbpol.2020.117181

Mallakuntla, M. K., Vaikuntapu, P. R., Bhuvanachandra, B., Podile, A. R. (2020). Selection and mutational analyses of the substrate interacting residues of a chitinase from Enterobacter cloacae subsp. cloacae (EcChi2) to improve transglycosylation. *International Journal of Biological Macromolecules 165*, 2432-2441. https://doi.org/10.1016/j.ijbiomac.2020.10.125

Manavalan, P., Johnson Jr, W. C. (1983). Sensitivity of circular dichroism to protein tertiary structure class. *Nature 305*(5937), 831-832. https://doi.org/10.1038/305831a0

Rojas-Osnaya, J., Rocha-Pino, Z., Nájera, H., González-Márquez, H., Shirai, K. (2020). Novel transglycosylation activity of *β-N*-acetylglucosaminidase of *Lecanicillium lecanii* produced by submerged culture. *International Journal of Biological Macromolecules 145*, 759-767. https://doi.org/10.1016/j.ijbiomac.2019.12.237

Seidl, V. (2008). Chitinases of filamentous fungi: a large group of diverse proteins with multiple physiological functions. *Fungal Biology Reviews 22*(1), 36-42. https://doi.org/10.1016/j.fbr.2008.03.002

Sreerama, N., Venyaminov, S. Y., Woody, R. W. (2000). Estimation of protein secondary structure from circular dichroism spectra: inclusion of denatured proteins with native proteins in the analysis. *Analytical Biochemistry 287*(2), 243-251. https://doi.org/10.1006/abio.2000.4879

Taira, T., Fujiwara, M., Dennhart, N., Hayashi, H., Onaga, S., Ohnuma, T., Fukamizo, T. (2010). Transglycosylation reaction catalyzed by a class V chitinase from cycad, *Cycas revolute*: a study involving site-directed mutagenesis, HPLC, and real-time ESI-MS. *Biochimica et Biophysica Acta (BBA)-Proteins and Proteomics 1804*(4), 668-675. https://doi.org/10.1016/j.bbapap.2009.10.015

Tronsmo, A., Harman, G. E. (1993). Detection and quantification of *N*-acetyl-*β*-D-glucosaminidase, chitobiosidase, and endochitinase in solutions and on gels. *Analytical Biochemistry 208*(1), 74-79. https://doi.org/10.1006/abio.1993.1010

Umemoto, N., Ohnuma, T., Osawa, T., Numata, T., Fukamizo, T. (2015). Modulation of the transglycosylation activity of plant family GH18 chitinase by removing or introducing a tryptophan side chain. *FEBS Letters 589*(18), 2327-2333. https://doi.org/10.1016/j.febslet.2015.07.018

Wallace, B. A., Janes, R. W. (2001). Synchrotron radiation circular dichroism spectroscopy of proteins: secondary structure, fold recognition and structural genomics. *Current Opinion in Chemical Biology 5*(5), 567-571. https://doi.org/10.1016/S1367-5931(00)00243-X

Whitmore, L., Wallace, B. A. (2004). DICHROWEB, an online server for protein secondary structure analyses from circular dichroism spectroscopic data. *Nucleic Acids Research 32*(suppl. 2), W668-W673. https://doi.org/10.1093/nar/gkh371

Whitmore, L., & Wallace, B. A. (2008). Protein secondary structure analyses from circular dichroism spectroscopy: methods and reference databases. *Biopolymers: Original Research on Biomolecules 89*(5), 392-400. https://doi.org/10.1002/bip.20853

Yang, S., Song, S., Yan, Q., Fu, X., Jiang, Z., Yang, X. (2014). Biochemical characterization of the first fungal glycoside hydrolyase family 3 *β-N*-acetylglucosaminidase from *Rhizomucor miehei. Journal of Agricultural and Food Chemistry 62*(22), 5181-5190. https://doi.org/10.1021/jf500912b

Zapata-Luna, R.L., Davidov-Pardo, G., Pacheco, N., Ayora-Talavera, T., Espinosa-Andrews, H., García-Márquez, E., Cuevas-Bernardino, J.C. (2023). Structural and physicochemical properties of bio-chemical chitosan and its performing in an active film with quercetin and *Phaseolus polyanthus* starch. *Revista Mexicana de Ingeniería Química 22*(2), 1-7. https://doi.org/10.24275/rmiq/Alim2315